MICHIGAN STATE
UNIVERSITY

National Superconducting Cyclotron Laboratory

NUMERICAL TECHNIQUE TO DETERMINE LONGITUDINAL FIELDS OF BUNCHED BEAMS WITHIN CONDUCTING BOUNDARIES

L.G. VOROBIEV and R.C. YORK

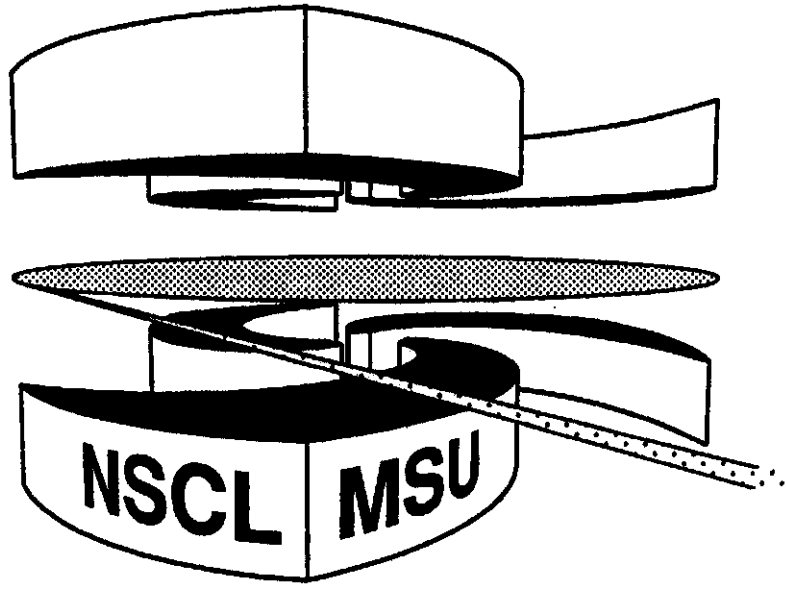

MSUCL-1117 OCTOBER 1998

NUMERICAL TECHNIQUE TO DETERMINE LONGITUDINAL FIELDS OF BUNCHED BEAMS WITHIN CONDUCTING BOUNDARIES

L.G.Vorobiev and R.C.York

National Superconducting Cyclotron Laboratory
Michigan State University
East Lansing, MI 48824

Abstract

A technique for computing the longitudinal electric fields of a bunched beam propagating inside a conducting pipe is presented. A beam bunch is represented as a series of discs or slices, and the total electrical field is found by superposition of the fields of individual slices. The results of this technique are shown to agree well with analytical models and other independent algorithms. The primary motivation for developing this technique was to provide an efficient and accurate calculational approach for the simulation of the longitudinal dynamics in sub-3D codes in lieu of a straightforward Poisson Solver. However the formalism may be employed in other applications to find electric fields for various beam particle distributions in the presence of conducting boundaries.

1. Introduction

Simulations including the effects of space charge provide a crucial basis for the design of high-current accelerator systems. In some cases, particularly for unbunched beams, two-dimensional (2-D) beam simulation particle-in-cell (PIC) codes are often sufficient. However, for the case of bunched beams, the longitudinal effects can become important, and 3-D or nearly 3-D simulations are required.

The general 3-D PIC methods provide completely self-consistent models, but frequently require very long computational times. As a result, the exploration of possible design space can, as a practical matter, be limited. An alternative approach is the modification of a 2-D PIC formulation to include important aspects of the longitudinal dynamics. The general intent is to create a simulation package that, while not as complete as a general 3-D PIC approach, will nevertheless have a nearly complete physics model and a computational speed which dramatically exceeds the general 3-D approach.

A simple linear model of the longitudinal electrical field, corresponding to parabolic line charge density, is valid for bunched elliptical beams in free space. However, in the presence of a conducting beam chamber with dimensions comparable to the beam transverse dimensions, the longitudinal electric field becomes non-linear due to image charges and common approximations are inappropriate. The non-linearity becomes especially apparent for the case of long or longitudinally-asymmetric bunches within a conducting beam pipe.

This paper describes a fast and accurate computational approach for the calculation of the longitudinal electrical field of beams with a relatively arbitrary charge density distribution within a conducting boundary. We believe the proposed method provides a unique strategy for the inclusion of longitudinal dynamics into the PIC codes.

2. Basic Formulae

2.1 Green's Function

To calculate in the beam coordinate frame the space charge electric fields of a bunched beam propagating inside a conducting cylinder, a common analytical approach is to find the solution of the Poisson equation.

$$\begin{cases} \Delta u = -4\pi\rho(\mathbf{r}) , & \mathbf{r} \in \Re \\ u(\mathbf{r})\big|_{\mathbf{r}\in\partial\Re} = 0 \end{cases} \tag{1}$$

The domain $\Re$ represents a grounded cylinder of infinite longitudinal (z) extent and $\partial\Re$ denotes the cylinder surface at radius $r = R_{cyl}$. Using the Green's function method[1], the potential can be expressed by the integral:

$$u(\mathbf{r}) = \int_{\Re} G(\mathbf{r},\mathbf{r}')\rho(\mathbf{r}')dV(\mathbf{r}') \quad \text{with} \quad \mathrm{r} = (x, y, z) \tag{2}$$

where $G(\mathrm{r}, r')$ represents the three-dimensional Green's function in Cartesian coordinates. For rectangular or free space regions, calculation of the potential from the convolution integral (2) is relatively fast and convenient[2]. However, with the inclusion of a conducting cylindrical surface, the function $G(\mathrm{r}, r')$ satisfying zero boundary conditions has a complicated form, and another approach should be considered.

From the Laplacian operator in cylindrical variables,

$$\Delta_{r,\varphi,z} u = \frac{\partial^2}{\partial r^2} + \frac{1}{r}\frac{\partial}{\partial r} + \frac{1}{r^2}\frac{\partial^2}{\partial \varphi^2} + \frac{\partial^2}{\partial z^2}$$

a specific form of the Green's function in cylindrical coordinates may be found that satisfies the zero boundary conditions on the cylinder surface by expanding $1/(\mathrm{r}-\mathrm{r}')$ using Bessel functions.

In the absence of the boundary surface, the expansion of the Green's function[1] is:

$$G(\mathrm{r},\mathrm{r}') = \frac{2}{\pi}\sum_{m=-\infty}^{\infty}\int_0^{\infty} dk \cdot e^{im(\varphi-\varphi')}\cos k(z-z')I_m(kr_<)K_m(kr_>) \qquad (3)$$

where $I_m(kr_<)$ and $K_m(kr_>)$ are the modified Bessel functions and

$$r_{<,>} = \begin{cases} \mathbf{r}', & \text{if } \mathbf{r}' <,> \mathbf{r} \\ \mathbf{r}, & \text{if } \mathbf{r} <,> \mathbf{r}' \end{cases}$$

To implement the conducting cylinder boundary with radius R_{cyl}, the Green function will be written as (reference 3):

$$G(\mathbf{r},\mathbf{r}') = \frac{2}{\pi}\sum_{m=-\infty}^{\infty}\int_0^{\infty} dk \cdot e^{im(\varphi-\varphi')}\cos k(z-z')\frac{I_m(kr_<)}{I_m(kR_{cyl})}[I_m(kR_{cyl})K_m(kr_>) - I_m(kr_>)K_m(kR_{cyl})] \quad (3)'$$

and the potential as:

$$u(\mathrm{r}) = \int_V G(\mathrm{r},\mathrm{r}')\rho(\mathrm{r}')dV(\mathrm{r}') \quad \text{with} \quad \mathrm{r} = (r,\varphi,z) \quad (2)'$$

Equation (3)′ has been used as a starting point for a series of further simplifying assumptions such as, for example, symmetrical charge density distributions, constant envelope sizes, asymptotic cases for $z \to \infty$, etc. (See, for example, references 1 and 3.) However, even for relatively common situations as e.g., a uniformly populated ellipsoid in a cylindrical pipe, the parameters k and z' are mixed in the arguments of the functions I_m, K_m. Therefore, a simple analytical evaluation of the integral (2)′ by Fourier transformation is not possible and numerical methods are required.

A straightforward approach often used in PIC codes is a numerical Poisson Solver in Cartesian or cylindrical coordinates[4,5]. This method can accommodate very general beam distributions and chamber boundaries while maintaining the self-consistency of the particle modeling. However, at each step along the beam path, the time-consuming procedure of calculating the grid density is required. Once the grid density is determined, the grid potentials can be found quite rapidly, usually employing the FFT technique.

Our approach remains related to the Green's function formalism, is based on the charge density method, and is also appropriate for PIC simulation.

2.2 Charge Density Method

For the free space potential (2) in Cartesian coordinates, the specific form of the Green's

function is $1/\mathbf{R}$ and the potential can be rewritten as:

$$u(\mathbf{r}) = \int_V \frac{\rho(\mathbf{r}')}{\mathbf{R}} dV(\mathbf{r}'), \quad \text{with} \quad \mathrm{R} = |\mathrm{r} - \mathrm{r}'| = \sqrt{(x-x')^2 + (y-y')^2 + (z-z')^2} \qquad (4)$$

The expression (4) in the free space may be written as:

$$u(x_0, y_0, z_0) = \int_{-Z_b}^{+Z_b} \int_0^{2\pi} \int_0^{R(z,\varphi)} \frac{\rho(r,\varphi,z)\, r dr\, d\varphi\, dz}{\sqrt{(r\cos\varphi - x_0)^2 + (r\sin\varphi - y_0)^2 + (z-z_0)^2}} \qquad (5)$$

where for the particular case of an ellipsoid-like bunch $R(z,\varphi) = R_b\sqrt{1-(z/Z_b)^2}$ (with R_b and Z_b are bunch radius and length correspondingly).

If the charge density ρ is given, then equation (5) determines the corresponding potential u. Conversely, if the potential u is known, then the corresponding charge density ρ may be found from (5) as an integral equation. In our method, we use both options. The formalism known as the moment method described below is from reference 6. A similar technique called the charge density method is commonly used in electron and ion optics[7]. Both approaches are based on dividing the volume of integration into discrete cells and assuming that the charge density within each cell is constant. As a result, the original integral equation (5) to find ρ for given u is reduced to the solution of a set of linear equations.

The charge density technique is especially efficient when the conducting boundary and the particle density distribution have symmetries. We use such simplifications in the computational schemes below.

3. Discrete Representation Of Beam Bunch: Slice Formalism

This section discusses the technique for a single slice in the presence of a conducting boundary.

3.1 Charge Density Method (Discretization)

The full beam bunch may be represented as a sequence of thin charged disks or slices, each with a charge density $\sigma^{slice}(r)$ (E.G. constant, Gaussian etc.) For a single slice of radius R_{slice}, the potential equation (5) can be expressed as:

$$u(x_0, y_0, z_0) = \int_0^{2\pi} \int_0^{R_{slice}} \frac{\sigma^{slice}(r)\, r dr\, d\varphi}{\sqrt{(r\cos\varphi - x_0)^2 + (r\sin\varphi - y_0)^2 + z_0^2}} \qquad (6)$$

Where the integration over z is not required for the infinitesimally thin slice. If the point (x_0, y_0, z_0) is on the cylindrical surface, then $x_0^2 + y_0^2 = R_{cyl}^2$ and $u(x_0, y_0, z_0) = u(r = R_{cyl}, z_0)$.

For numerical evaluations, the area of integration in (6) may be sub-divided and the integral may be represented as a discrete sum:

$$u(x_0, y_0, z_0) = h_\varphi h_R \sum_{j=0}^{N_\varphi} \sum_{k=0}^{N_R} \frac{\sigma_k^{slice} r_k}{\sqrt{(r_k \cos\varphi_j - x_0)^2 + (r_k \sin\varphi_j - y_0)^2 + z_0^{\,2}}} \tag{7}$$

where $h_\varphi = 2\pi / N_\varphi$, $h_R = R_b / N_R$ and σ_k^{slice} is a surface charge density of the slice.

Equation (7) defines the potential on the cylindrical surface due to a single slice at longitudinal position z_0. The same potential evaluated at the position of the conducting boundary (r ≡ R_{cyl}), but with opposite sign, is used to find the surface image charge density σ^{image} on the cylinder:

$$-u(x_0, y_0, z_0) = h_\varphi h_Z \sum_{i=1}^{N_Z} \sigma_i^{image} \left\{ \sum_{j=0}^{N_\varphi} \frac{R_{cyl}}{\sqrt{(R_{cyl} \cos\varphi_j - x_0)^2 + (R_{cyl} \sin\varphi_j - y_0)^2 + (z_i - z_0)^2}} \right\} \tag{8}$$

where $h_Z = 2Z_L / N_Z$, $z_0 \in [-Z_L, Z_L]$ with $Z_L = 4Z_b$.

Both the charge density and moment methods (See references 6 and 7) are based on the fact that if the potential $u(\mathbf{r}_0)$ is given as a set of values, then the charge density may be found as a solution of a set of linear equations (8) where the value within the { } brackets are the matrix coefficients. We use this scheme below.

3.2 On-axis Potential

The on-axis $(x_0^2 + y_0^2 = 0)$ potential for a single slice of radius R_b and $\sigma^{slice}(r) \equiv const$ can from equation (6) be expressed analytically:

$$u_{on-axis}^{slice}(z) = \int_0^{2\pi} \int_0^{R_b} \frac{\sigma^{slice} \cdot r dr d\varphi}{\sqrt{r^2 + z^2}} = 2\pi\sigma^{slice} \left(\sqrt{R_b^{\,2} + z^2} - |z| \right) \tag{9}$$

where we assume that the slice is at the longitudinal position $z = 0$. For $z \to \pm\infty$, equation (9) reduces to the potential for a point-charge $u_{on-axis}^{slice} = Q/|z|$, where $Q = \pi R_b^{\,2} \sigma^{slice}$ is the total electrical charge of the slice.

3.3 Computational Scheme for a Single Slice

Given the image potential on the cylinder axis, the total field is the sum of $u^{slice}_{on-axis}$ and $u^{image}_{on-axis}$. The image potential is found by the following steps.

1. The free space potential $u^{slice}_{free}(r,z)$ from each slice on a cylindrical surface for $r=\sqrt{x_0^2+y_0^2}=R_{cyl}$ is found from the general expression (7).

2. Substituting the free space potential with opposite sign $-u^{slice}_{free}(r=\sqrt{x_0^2+y_0^2}=R_{cyl},z)$ into the set of linear equations (8), the image density distribution $\sigma^{slice}_{image}(r=\sqrt{x_0{}^2+y_0{}^2}=R_{cyl},z_i)$ is found as a solution of the set of linear equations. This procedure guarantees that the total potential will be zero on the cylinder wall: $u^{slice}_{total}(r=R_{cyl},z)=0$.

3. Given the image charge density, the corresponding image potential $u^{slice}_{image}(x_0,y_0,z_0)$ is obtained by reapplication of formula (8) with $\sigma^{slice}_{image}(R_{cyl},z_i)$ and $x_0^2+y_0^2=0$. (This technique may also be used to calculate the off-axis $(x_0^2+y_0^2\neq 0)$ potential as discussed in Section 4.3.)

4. The total slice potential is simply the sum of the image charge and free space potentials $(u^{slice}_{total}(r,z)=u^{slice}_{free}(r,z)+u^{slice}_{image}(r,z))$. (Note that for the on-axis case $(r=0)$ $u^{slice}_{free}(0,z)=u^{slice}_{on-axis}(z)$)

This approach can be used to calculate both on- and off-axis potentials of each slice at the conducting boundary. The potentials $u^{slice}_{total}(r,z)$ can be found for slices with various radii and non-uniform (e.g. Gaussian) charge densities. The total bunch potential $u^{bunch}_{total}(r,z)$ is a result of superposition, integrating all $u^{slice}_{total}(r,z)$ over $z\in[-Z_L,Z_L]$.

When this procedure is applied to a PIC code, it is proposed that the potentials and electrical field values be calculated once and stored. During the simulation, these values with interpolation would be used to provide an accurate model of the longitudinal dynamics without the penalty of long computational time.

4. Numerical Examples

In the numerical examples below, we consider in Section 4.1 an elliptical beam bunch propagating through a conducting cylindrical pipe with different values of the ratio of bunch radius to bunch length. In Section 4.2, we compute the case of a beam bunch with

a longitudinally asymmetric charge density distribution. Finally, in Section 4.3, we evaluate the off-axis longitudinal fields that, for the case considered, show a weak radial dependence.

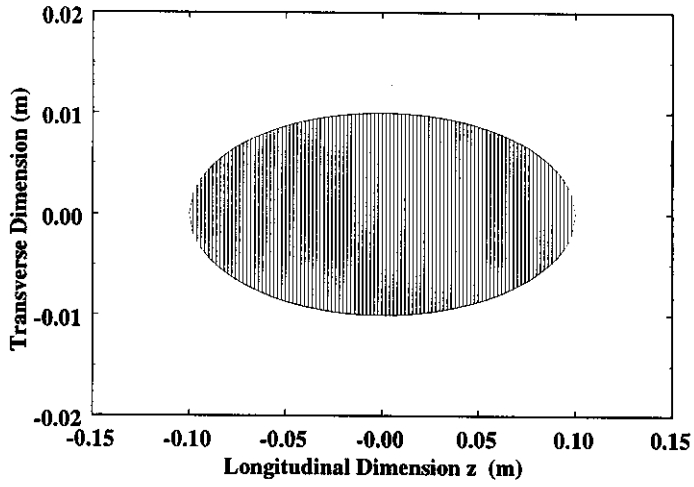

Figure 1. A uniformly populated ellipsoidal beam bunch modeled as 100 discrete slices. The bunch radius is R_b=0.01 m and the half bunch length is Z_b=0.1 m.

4.1 Ellipsoidal Bunch with Uniform Charge Density in a Cylindrical Pipe

We consider a specific case of an elliptical bunch inside a conducting cylindrical pipe of radius 0.02 m as shown in Figure 1. The half bunch length, Z_b is 10 cm, the maximum transverse radius R_b is 1 cm, and the total charge is $Q_{total} = 10^{-11}$ C. The transverse dimensions of the beam were assumed circular with a uniform radial charge distribution. The longitudinal dimension was assumed parabolic thus resulting in a parabolic line charge density $\lambda(z)$. In this example, the bunch was modeled as 100 individual slices.

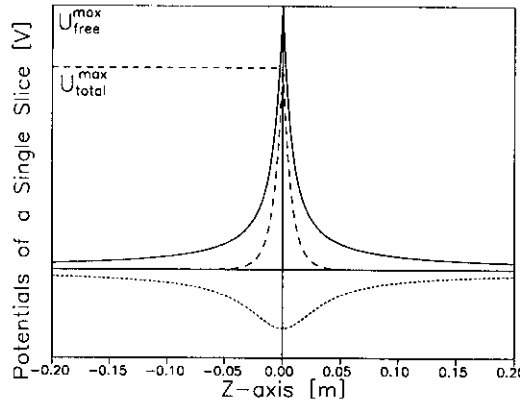

Figure 2. The longitudinal potentials in arbitrary units for the middle (z = 0) slice of Figure 1. The solid, dotted, and dashed curves are the free space, image charge, and total potential respectively.

The longitudinal potential, u(z) for the middle slice (z = 0) is plotted in Figure 2, where the potentials for free space, image, and total are shown. Note that the slope of the total potential is greater than that of the free space potential due to image charges. For the full bunch in the absence of the conducting chamber, superposition of the free space potentials for all slices results in the u(z) and $E_z(z)$ given in Figure 3. Note that the resulting field $E_z(z)$ is linear within the bunch as would be predicted[8,9]. With the inclusion of a conducting cylinder, superposition of the total potentials for all slices results in u(z) and $E_z(z)$ given in Figure 4. Note that, for this case, the $E_z(z)$ within the bunch is non-linear.

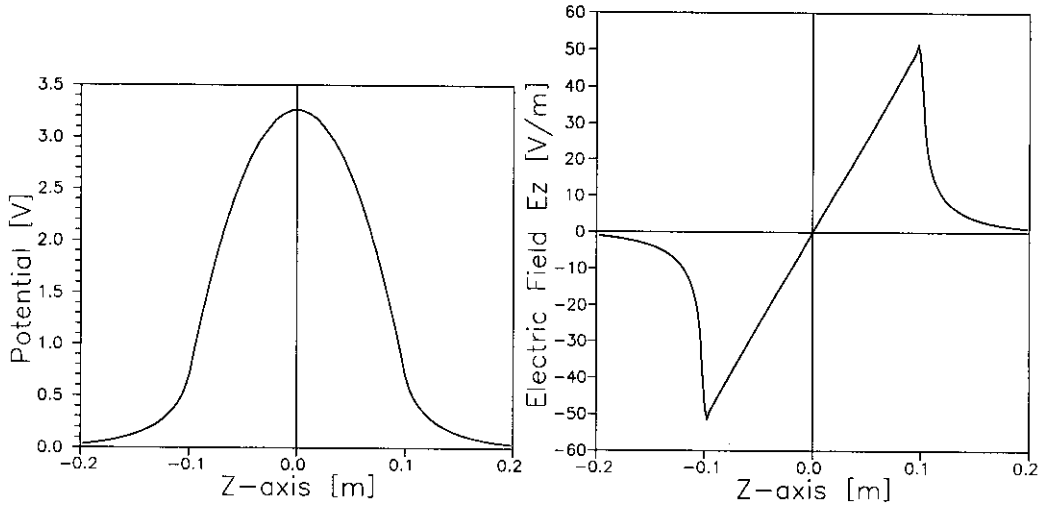

Figure 3. The u(z) [V] and $E_z(z)$ [V/m] in free space for the beam bunch of Figure 1.

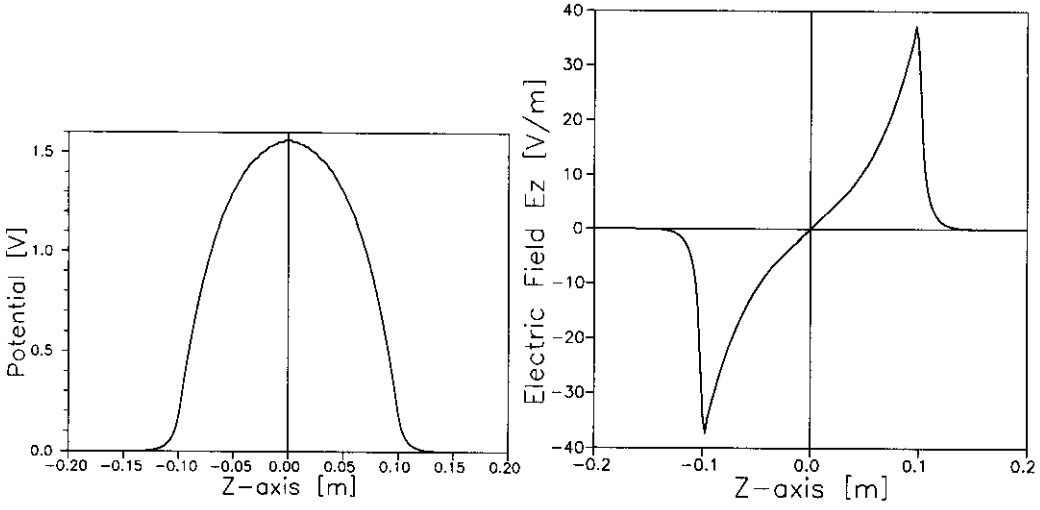

Figure 4. The longitudinal potential u(z) [V] and electric field $E_z(z)$ [V/m] along the beam axis from superposition of 100 slices for the case of the ellipse-like bunch (length / diameter = 10) within a metal cylinder beam pipe 4 cm in diameter.

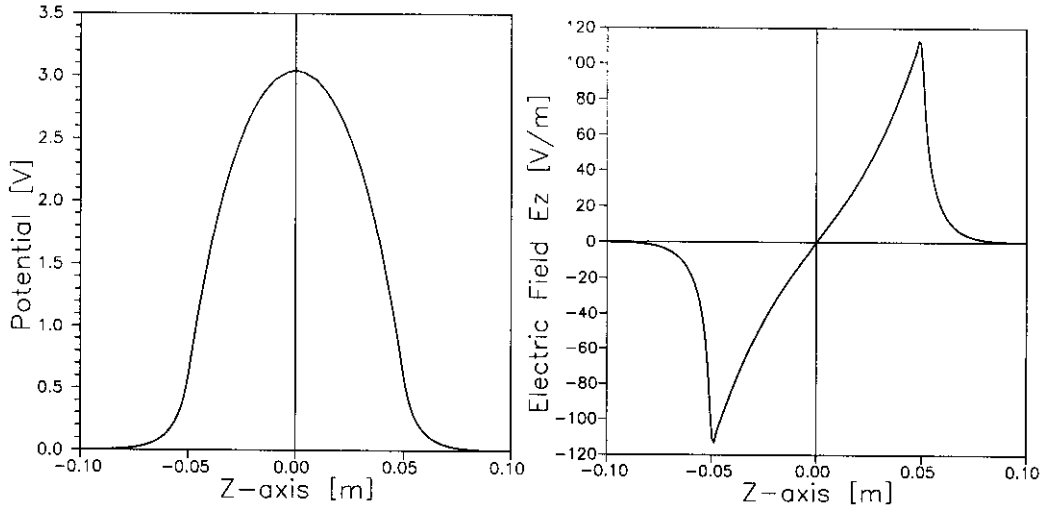

Figure 5. The longitudinal potential u(z) [V] electric field $E_z(z)$ [V/m] found by superposition of 100 slices for the case of the bunch length / diameter = 5.

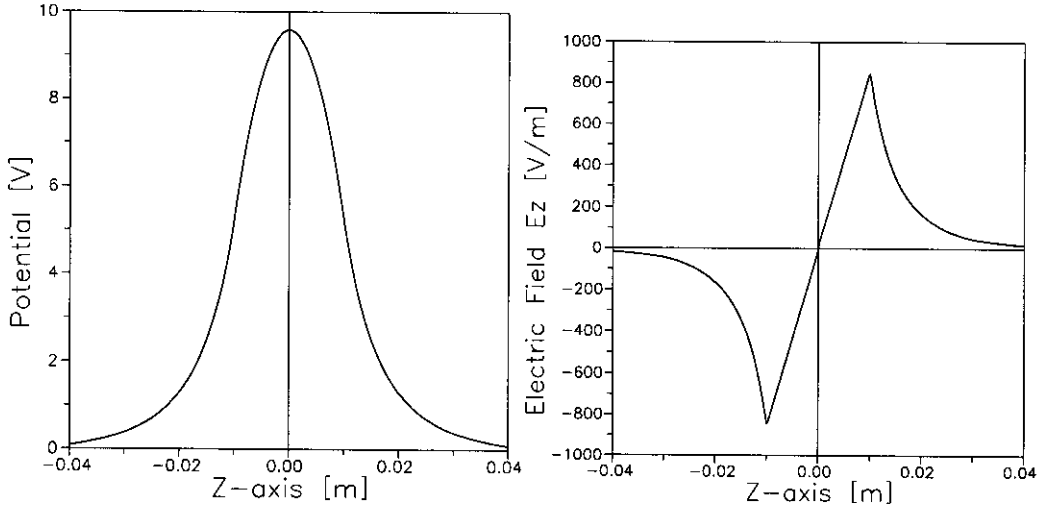

Figure 6. The longitudinal potential u(z) [V] and electric field $E_z(z)$ [V/m] found by superposition of 100 slices for the case of the length / diameter = 1 (spherical bunch). For such a short bunch, the total electric field remains linear (See reference 9).

A number of cases for the bunch relative to the conducting chamber dimensions were evaluated. Specifically, the bunch length to chamber radius values of 10, 5, and 1 were calculated. (See Figure 4 through Figure 6.) Our results are in agreement with the same cases presented in reference 9 page 407.

4.2 Asymmetrical Bunch in Cylindrical Pipe

More complicated situations, such as when the bunch has a non-symmetrical form in the longitudinal direction, can not be adequately represented by the g-factor method. However, the proposed approach may accommodate such cases. For example, shown in Figure 7, is a possible asymmetrical bunch within a 4 cm diameter conducting pipe again modeled as 100 individual slices with the calculated u(z) and $E_z(z)$ given in Figure 8.

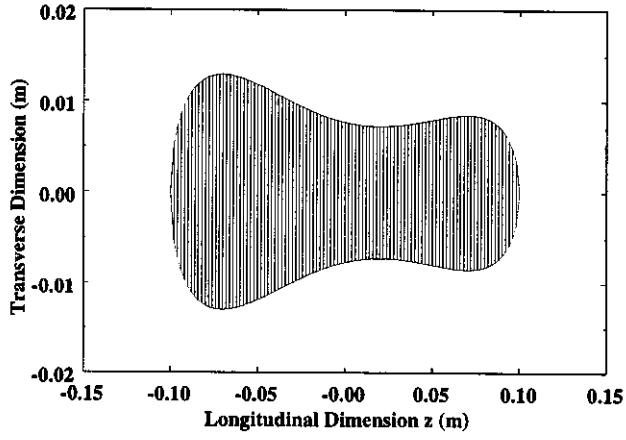

Figure 7. Asymmetrical bunch within a conducting beam pipe 4 cm in diameter.

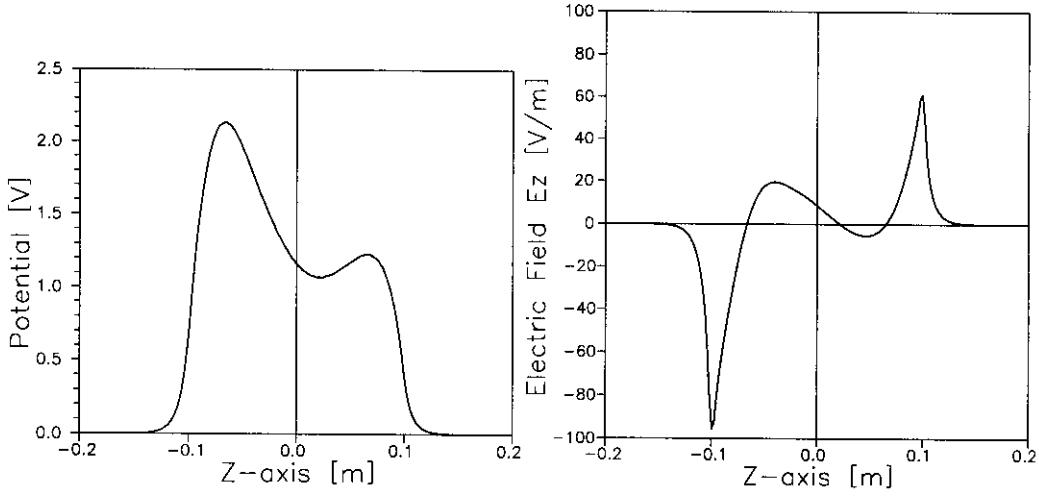

Figure 8. Longitudinal potential on-axis u(z) [V] and field $E_z(z)$ [V/m] found by slice superposition for the asymmetrical bunch of Figure 7.

Though the geometrical shape of the bunch of Figure 7 is not dramatically different from that of Figure 1, the electric potential and field have significantly different profiles. The $E_z(z)$ of the elliptical bunch from Figure 1 is only modestly non-linear within the bunch

(See Figure 4) whereas the $E_z(z)$ of Figure 8 changes sign four times. The g-factor averaging method in this case would lead to the wrong result.

4.3 Off-axis Electrical Field

So far we have assumed that $E_z(z)$ is independent of radial position and that the beam is concentric with the conducting boundary. Shown in Figure 9 are the potentials and fields for different radial positions.

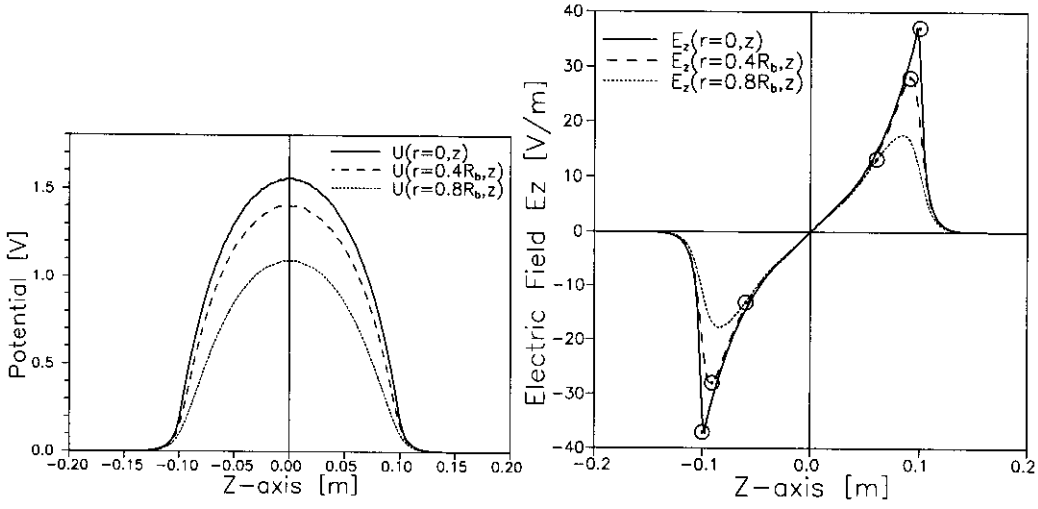

Figure 9 The dependence of the potential u(r,z) [V] and the field $E_z(r,z)$ [V/m] as a function of z for r = (0, 0.4 and 0.8)$\times R_b$ [m]. The symbols in the E_z plot denote the maximum z value of the bunch at the specific radius. The bunch dimensions are the same as those of Figure 1.

From Figure 9, the approximation of simply using the on-axis value for $E_z(z)$ will cause significant errors only near the bunch ends. However, the maximum $Z_{max}(r)$ values for the example shown are $Z_{max}\{r = (0, 0.4, 0.8)\times R_b\} = 0.1, 0.09, 0.06$ m. (The symbols are plotted at these Zmax values in Figure 9.) I.E., there are few or no particles in the area of significant deviation from the on-axis value for $E_z(z)$. Since $E_z(r,z)$ can be found by interpolation from tabulated data generated by computations performed at the beginning of each simulation, the computational time penalty will be relatively modest should the inclusion of the E_z radial dependence be desirable.

5. Discussion and Conclusions

We plan to employ the presented technique to include the longitudinal dynamics as part of an upgrade to an existing 2-D PIC code. The transverse dynamics will be modeled by "representative" slices that have a population consisting of particles within the range of longitudinal z coordinates suitable for each slice with the appropriately scaled transverse charge density. Initially, the longitudinal dynamics will be calculated assuming a cylindrical vacuum pipe and will be based on the slice technique. Though not specifically

discussed, it should be noted that the procedure presented can be used to accommodate more general chamber boundaries and beam shapes and this generalization is planned.

Since for each slice the total potential is simply the sum of the free space and image potentials, the superposition of these potentials representing the whole will automatically satisfy the conducting chamber boundary conditions. To reduce simulation time, a range of slice geometries (in the simplest case – a range of discs of different radii) will be calculated and tabulated. The required number of these "template" slices is normally an order of magnitude less than the number of slices representing the bunch. In the examples presented, approximately 15 different slice configurations were used requiring a computational time of about 5 minutes (on a multi-user 433 MHz DEC Alpha).

The example bunch configurations were modeled as 100 distinct slices with the potential for each slice derived from appropriate interpolation of the tabulated data and scaling for charge density. The number of slices N_{slice} as well as N_Z, N_φ, N_R in (7)-(8) are variables that may be set appropriate to the problem under consideration. Usually it is chosen to approximate the integral (6) by the discrete sums with accuracy sufficient and to suppress ripple in the total potential after the superposition procedure. The construction of the total bunch potential from the 100 individual slice values required only about 0.2 s.

Since the pre-simulation calculations (about 5 minutes) need only be done once while the accelerator simulations require many computations of the total bunch potential (about 0.2 s) as the particles are tracked through the system, the decrease in overall computational time will be enormous.

We are aware that the proposed sub-3-D PIC code will not be completely self-consistent since the planned pre-simulation calculational procedure will be unable to reflect all possible evolutions of the particle density. However, preliminary studies of the radial dependence of Ez field for different distributions suggests that the effect of variations in the transverse charge distribution is minor, and therefore, the analysis will be nearly self-consistent. Comparisons with the results of more general 3-D codes such as WARP-3D are planned[10].

Acknowledgements

The authors are grateful to Felix Marti for useful discussions.

References

[1] J.D.Jackson "Classical Electrodynamics", 2-nd Edition, John Wiley & Sons (1975), New York, pp. 116-118.

[2] L.G. Vorobiev and K. Hirata, "A Sympletic Poisson Solver Based on Fast Fourier Transformation", KEK Report 95-12 (November 1995).

[3] E.Henestroza "Longitudinal Electric field inside a beam with non-uniform radius", HIFAR Note 379, LBNL, Berkeley.

[4] L.G.Vorobiev "Rapid Poisson Solver based on FFT for domain with various boundary conditions", Preprint ITEP-193, Moscow (1984).

[5] L.G. Vorobiev, "Two-dimensional particle code for beam simulation in HIF driver", Preprint ITEP 22-94, Moscow (1994).

[6] R.E. Harrington, "Field Computation by Moment Methods", Macmillan Company, New York, (1968).

[7] M.Szilagyi "Electron and Ion Optics", Plenum Press, New York (1988).

[8] C. Allen, N. Brown and M. Reiser, "Image Effects for Bunched Beams in Axisymmetric Systems", Particle Accelerators, **45** (1994) 146-165.

[9] M. Reiser, "Theory and Design of Charge Particle Beams", John Wiley & Sons, New York (1994).

[10] D.P.Grote, A.Friedman and I.Haber "Three dimensional PIC simulation of heavy ion fusion beams: recent Improvements to and applications of WARP", PAC-93, vol. **1** (1993), 727-729.